



OPEN ACCESS

EDITED BY

Sethumathavan Vadivel,
Tokyo Institute of Technology, Japan

REVIEWED BY

Bulelwa Ntsendwana,
Mintek, South Africa
Zuzanna Bielán,
Institute of Fluid Flow Machinery (PAN),
Poland

*CORRESPONDENCE

Shahid Iqbal,
✉ shahid.i14@yahoo.com
Ali Bahadur,
✉ abahadur@wku.edu.cn
Eslam B. Elkaeed,
✉ ikaeed@mcast.edu.sa

SPECIALTY SECTION

This article was submitted to
Photocatalysis and Photochemistry,
a section of the journal
Frontiers in Chemistry

RECEIVED 17 December 2022

ACCEPTED 08 March 2023

PUBLISHED 19 April 2023

CITATION

Qamar MT, Iqbal S, Aslam M, Alhujaily A,
Bilal A, Rizwan K, Farooq HMU, Sheikh TA,
Bahadur A, Awwad NS, Ibrahim HA,
Almufarj RS and Elkaeed EB (2023),
Transition metal doped CeO₂ for
photocatalytic removal of 2-
chlorophenol in the exposure of indoor
white light and antifungal activity.
Front. Chem. 11:1126171.
doi: 10.3389/fchem.2023.1126171

COPYRIGHT

© 2023 Qamar, Iqbal, Aslam, Alhujaily,
Bilal, Rizwan, Farooq, Sheikh, Bahadur,
Awwad, Ibrahim, Almufarj and Elkaeed.
This is an open-access article distributed
under the terms of the [Creative Commons Attribution License \(CC BY\)](https://creativecommons.org/licenses/by/4.0/).
The use, distribution or reproduction in
other forums is permitted, provided the
original author(s) and the copyright
owner(s) are credited and that the original
publication in this journal is cited, in
accordance with accepted academic
practice. No use, distribution or
reproduction is permitted which does not
comply with these terms.

Transition metal doped CeO₂ for photocatalytic removal of 2-chlorophenol in the exposure of indoor white light and antifungal activity

M. Tariq Qamar¹, Shahid Iqbal^{2*}, M. Aslam³, Ahmad Alhujaily⁴, Anum Bilal², Komal Rizwan⁵, Hafiz Muhammad Umer Farooq⁶, Tahir Ali Sheikh⁷, Ali Bahadur^{8*}, Nasser S. Awwad⁹, Hala A. Ibrahim^{10,11}, Rasmiah S. Almufarj¹² and Eslam B. Elkaeed^{13*}

¹Department of Chemistry, Forman Christian College (A Chartered University), Lahore, Pakistan, ²Department of Chemistry, School of Natural Sciences (SNS), National University of Science and Technology (NUST), Islamabad, Pakistan, ³Centre of Excellence in Environmental Studies (CEES), King Abdulaziz University, Jeddah, Saudi Arabia, ⁴Biology Department, College of Science, Taibah University, Al Madinah Al Munawarah, Saudi Arabia, ⁵Department of Chemistry, University of Sahiwal, Sahiwal, Pakistan, ⁶Department of Chemistry, Government Islamia College, Civil Lines, Lahore, Pakistan, ⁷Department of Chemistry, The Islamia University of Bahawalpur, Bahawalpur, Pakistan, ⁸Department of Chemistry, College of Science and Technology, Wenzhou-Kean University, Wenzhou, China, ⁹Chemistry Department, Faculty of Science, King Khalid University, Abha, Saudi Arabia, ¹⁰Biology Department, Faculty of Science, King Khalid University, Abha, Saudi Arabia, ¹¹Department of Semi Pilot Plant, Nuclear Materials Authority, El Maadi, Egypt, ¹²Department of Chemistry, College of Science, Princess Nourah Bint Abdulrahman University, Riyadh, Saudi Arabia, ¹³Department of Pharmaceutical Sciences, College of Pharmacy, AlMaarefa University, Riyadh, Saudi Arabia

Besides natural sunlight and expensive artificial lights, economical indoor white light can play a significant role in activating a catalyst for photocatalytic removal of organic toxins from contaminated water. In the current effort, CeO₂ has been modified with Ni, Cu, and Fe through doping methodology to study the removal of 2-chlorophenol (2-CP) in the illumination of 70 W indoor LED white light. The absence of additional diffractions due to the dopants and few changes such as reduction in peaks' height, minor peak shift at 2θ (28.525°) and peaks' broadening in XRD patterns of modified CeO₂ verifies the successful doping of CeO₂. The solid-state absorption spectra revealed higher absorbance of Cu-doped CeO₂ whereas a lower absorption response was observed for Ni-doped CeO₂. An interesting observation regarding the lowering of indirect bandgap energy of Fe-doped CeO₂ (~2.7 eV) and an increase in Ni-doped CeO₂ (~3.0 eV) in comparison to pristine CeO₂ (~2.9 eV) was noticed. The process of e⁻–h⁺ recombination in the synthesized photocatalysts was also investigated through photoluminescence spectroscopy. The photocatalytic studies revealed the greater photocatalytic activity of Fe-doped CeO₂ with a higher rate (~3.9 × 10⁻³ min⁻¹) among all other materials. Moreover, kinetic studies also revealed the validation of the Langmuir-Hinshelwood kinetic model (R² = 0.9839) while removing 2-CP in the exposure of indoor light with a Fe-doped CeO₂ photocatalyst. The XPS analysis revealed the existence of Fe³⁺, Cu²⁺ and Ni²⁺ core levels in doped CeO₂. Using the agar well-diffusion method, the antifungal activity was assessed against the fungus *M. fructicola* and *F. oxysporum*.

Compared to CeO₂, Ni-doped CeO₂, and Cu-doped CeO₂ nanoparticles, the Fe-doped CeO₂ nanoparticles have outstanding antifungal properties.

KEYWORDS

modified CeO₂, band gap energy, photocatalytic removal, 2-chlorophenol, nanocomposite, antifungal activity

Introduction

A major environmental threat that humanity faces today is the contamination of water caused by hazardous chemicals released into the environment by industrial processes. Routine daily activities can cause hazardous materials to be introduced into natural water resources, such as aquifers, lakes, oceans, rivers, and groundwater aquifers. Continually introducing such contaminants into natural water can result in an alteration of the characteristic features of natural water as well as polluted water. This is extremely unsuitable for human health. Chemical pollutants like dyes for textiles, halogenated compounds, substituted phenols, insecticides, pesticides, weed killers, and herbicides are known to be carcinogenic and pose major health risks to humans (Anku et al., 2017; Samanta et al., 2019; Brillas and Garcia-Segura, 2020; Kanan et al., 2020; Rafiq et al., 2021). Among toxic organic pollutants-chlorophenols and nitrophenols, because of their stable structure, toxic and carcinogenic effects on the human being, have been a remaining area under concern (Chiou et al., 2008; Adewuyi et al., 2016; Umukoro et al., 2017; Sharma et al., 2019; Barakat et al., 2020). Therefore, it is highly desirable to remove these toxins effectively from the polluted water.

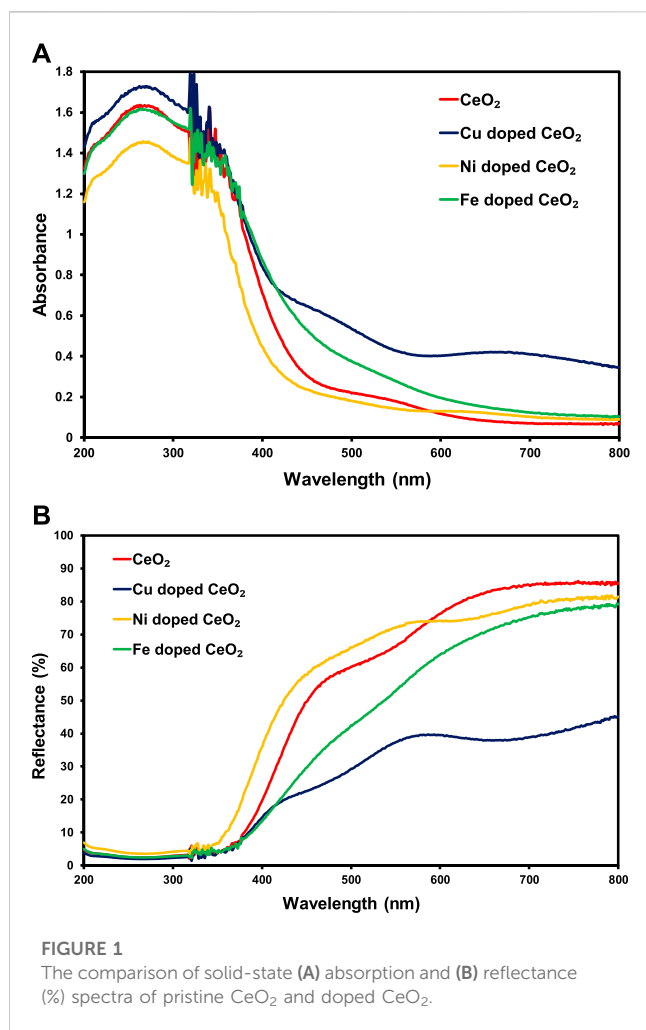
The structural properties of these phenols and their derivatives have made them difficult to remove from the polluted water by classical methods, i.e., activated carbon adsorption, chemical oxidation, and biological treatment. Because activated carbon adsorption leads to phase separation without degradation of injurious pollutants, the chemical oxidation method is unable to remove pollutants efficiently, and biological treatments are slow and pH and temperature dependent, while the advanced oxidation process seems to be better for effective removal of such sort of destructive pollutants using light (Eryilmaz and Genç, 2021; Ren et al., 2021; Saputera et al., 2021).

Advanced oxidation leads to the formation of highly reactive species which ultimately react with organic pollutants to degrade them successfully (Mazivila et al., 2019; Du and Zhou, 2021; Gallo-Cordova et al., 2021; Huang et al., 2021; Luo et al., 2021). Among advanced oxidation processes, photocatalytic degradation and mineralization are efficient methods of converting highly toxic organic pollutants to harmless species under ambient conditions using light and a photocatalyst through homogeneous or heterogeneous photocatalysis. In addition, heterogeneous photocatalysis is considered advantageous over homogeneous photocatalysis due to an easy retrievability of a catalyst from the reaction mixture and then the reusability of a catalyst (Gisbertz and Pieber, 2020). Following the concept of the advanced oxidation process, the heterogeneous photocatalytic reaction starts with the generation of H₂O₂, OH[•], O₂^{•-}, HOO[•] and H⁺ species by the absorption of a photon having energy equal to or greater than the band gap energy of the photocatalyst which is being used (Loeb

et al., 2019; Pandey et al., 2020; Serrà and Philippe, 2020; Danish et al., 2021). In addition, hydroxyl and superoxide anion radicals react with phenols, depending on the position and nature of substituent groups on phenols, to degrade them into some oxygenate intermediates and consequently, these oxygenates mineralize to their respective harmless species (Qamar et al., 2017a; Qamar et al., 2017b; Alhogbi et al., 2020).

Metal oxide-assisted photocatalytic wastewater treatment is a relatively prospective subject and growing rapidly to remove hazardous pollutants from contaminated water. In this context, metallic oxide semiconductors such as TiO₂, ZnO, Fe₂O₃, SnO₂, WO₃, Bi₂O₃, V₂O₅, Cu₂O, NiO, etc. have been studied extensively both in artificial and natural light sources to acquire pollution free water (Ahmed et al., 2010; Oturan and Aaron, 2014; Wang et al., 2014; Qamar et al., 2015; Zangeneh et al., 2015; Aslam et al., 2018). However, exploration of a potential photocatalyst for the effective removal of toxic pollutants from the wastewater has not over yet and researchers are paying attention to study the photocatalytic properties of CeO₂-based photocatalysts for the abatement of organic pollutants. Although, bare CeO₂ has wide application in electrocatalysis, solar cells, fuel cells and photocatalysis due to its high chemical stability, low toxicity and greater oxygen storage capacity (Ma et al., 2019; Fauzi et al., 2022). However, its performance in photocatalysis is unsatisfactory due to greater photo excitons' recombination, lower absorption cross-section of light spectrum and higher band gap (2.8–3.1 eV) energy (Ma et al., 2019; Fauzi et al., 2022). Therefore, it is a need to modify CeO₂ in order to increase its utilization as a photocatalyst for removal of organic toxins. The unique thing of this study is the introduction of transition metals into CeO₂ without significantly changing the cubic structure of CeO₂ photocatalyst for the removal of 15 ppm 2-chlorophenol in the illumination of 70 W indoor white light.

Previously, researchers utilized expensive artificial light sources such as solar simulator, Hg and Xe lamps for photocatalytic degradation of various organic toxins using variety of photocatalysts (Tang et al., 2004; Hao et al., 2015; Aslam et al., 2016; Xu et al., 2017). In addition, a few studies are available for the photocatalytic removal of 2-CP using CeO₂-based photocatalysts such as CeO₂, g-C₃N₄(0.94)/CeO₂(0.05)/Fe₃O₄(0.01), TiO₂-CeO₂-ZrO₂ (Aslam et al., 2016; García-Hernández et al., 2019; Rashid et al., 2019). However, various combinations of CeO₂ with metals, non-metals and photocatalysts such as Ag₂CO₃, rGO, CdS, AgBr, SrFe₁₂O₉, BiOCl, g-C₃N₄, Co₃O₄, etc., are reported for the photocatalytic removal of organic dyes, phenols and pharmaceutical ingredients (Ma et al., 2019; Yao et al., 2021; Fauzi et al., 2022). Moreover, literature reveals that a photocatalysis setup while using an economical 70 W indoor white light for the removal of 2-CP over the proposed composition of CeO₂-based photocatalysts has not been reported before.

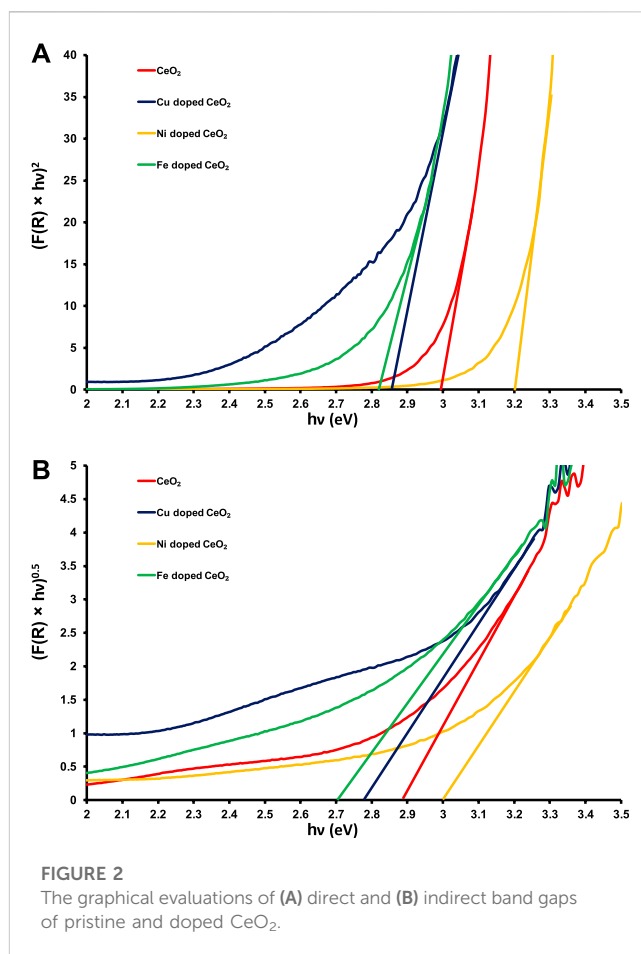


In this study, CeO₂ has been synthesized using a co-precipitation methodology and its modification was executed through doping with transition metals, i.e., Fe, Ni and Cu because 3d transition metals are considered capable dopants in tuning the properties of CeO₂ for catalysis applications (Yue and Zhang, 2009; Elias et al., 2014; Qi et al., 2019). The spectral response and bandgap of the synthesized materials were evaluated using UV-visible diffuse reflectance spectroscopy (UV-visible DRS) whereas photoluminescence (PL) fluorometer was used to investigate e^-h^+ recombination. X-ray diffraction (XRD) and X-ray photoelectron spectroscopy (XPS) were used to evaluate the structural and chemical characterization of synthesized materials. The photocatalytic activity of the synthesized photocatalysts was studied for the removal of 2-chlorophenol (2-CP) the kinetics for the photodegradation of 2-CP were also investigated.

Experimental

Materials

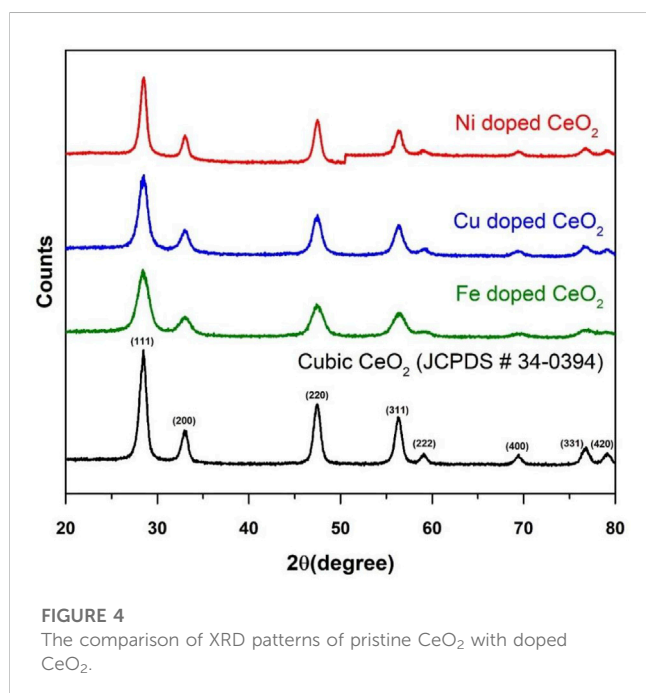
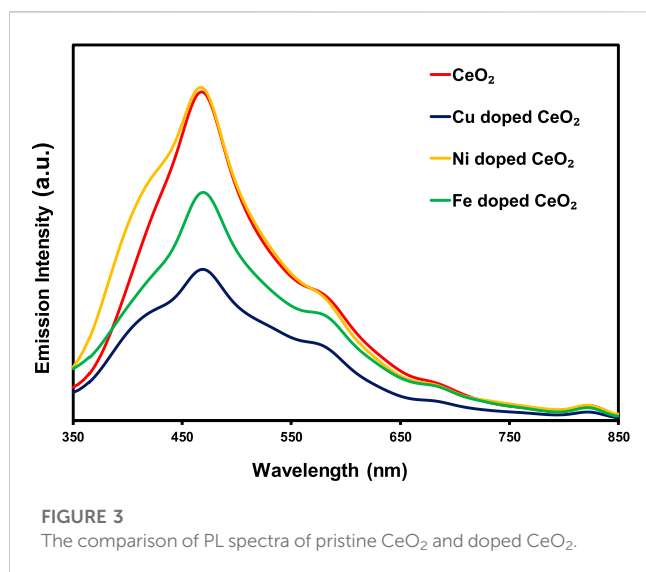
Cerium (III) nitrate hexahydrate [Ce(NO₃)₃·6H₂O, Sigma-Aldrich, ≥99%], iron (III) nitrate non-hydrate [Fe(NO₃)₃·9H₂O,



Sigma-Aldrich, 99.95%), nickel (II) nitrate hexahydrate [Ni(NO₃)₂·6H₂O, Sigma-Aldrich, ≥99%], copper (II) nitrate trihydrate [Cu(NO₃)₂·3H₂O, Sigma-Aldrich, 99.99%], ethanol (C₂H₅OH, Sigma-Aldrich, ≥99.8%), nitric acid [HNO₃, Sigma-Aldrich, 70%], acetone [CH₃COCH₃, Sigma-Aldrich], potassium hydroxide [KOH, Sigma-Aldrich, 99.5%] and triton X-100 [Tx-100, Sigma-Aldrich] were used without further purification for the synthesis of photocatalysts.

Synthesis of pristine CeO₂

In a typical synthesis of CeO₂, 30 g Ce(NO₃)₃·6H₂O was dissolved in 100 mL distilled water with continuous stirring until the formation of a clear solution. After complete dissolution, 3 mL Triton X-100 was added to the clear solution under continuous stirring for 30 min at room temperature. To hydrolyze the solution, 0.1M potassium hydroxide (KOH) was added to the solution dropwise till the formation of yellow precipitate near pH 9 at 50°C. The mixture containing the yellow precipitate, surfactant and KOH content was washed several times with distilled water and then with ethanol/water (30:60) mixture to remove surfactant and basic contents present in the mixture until the mixture attained the neutral pH. The precipitate was separated from the reaction mixture through filtration and the obtained yellow precipitate was again washed with ethanol/water (30:60) mixture and dried overnight at 100°C in a vacuum oven



and then calcined in a muffle furnace for 4 h at 400°C. The calcined material was ground using mortar and pestle to get fine powder of CeO₂ photocatalyst.

Synthesis of modified CeO₂

For the synthesis of Cu doped CeO₂, 0.381 g Cu(NO₃)₂·3H₂O and 30.681 g Ce(NO₃)₃·6H₂O were dissolved separately in distilled water with continuous stirring at room temperature till the formation of clear solutions and marked solution A and B, respectively. Then, solution A was added slowly into the beaker having solution B with continuous stirring at 50°C for 10 min followed by the addition of 3 mL Triton X-100 under continuous

stirring for 30 min. The mixture of both precursors and surfactant was then hydrolyzed with the slow addition of 0.1M KOH till the formation of precipitate at pH 9. The formed precipitate was separated through filtration, washed with water and ethanol/water (30:60) mixture, and dried overnight in a vacuum oven at 100 °C. The dried sample was then subjected to the muffle furnace for calcination at 400°C for 4 h. The calcined material was ground using mortar and pestle to get fine powder of Cu doped CeO₂ photocatalyst. The same procedure was applied for the synthesis of Ni-doped CeO₂ and Fe-doped CeO₂ except for the different amounts of precursors, e.g., 0.496 g Ni(NO₃)₂·6H₂O and 0.723 g Fe(NO₃)₃·9H₂O about the Ni and Fe contents, respectively for 30.681 g of Ce(NO₃)₃·6H₂O. The synthesized photocatalytic materials were characterized by UV- visible diffuse reflectance spectroscopy (UV-Vis DRS), photoluminescence (PL), X-ray Diffraction (XRD), scanning electron microscopy (SEM) and X-ray photoelectron spectroscopy (XPS).

Photocatalytic studies

The photocatalytic performance of transition metal doped CeO₂ was studied for the removal of 15 ppm 2-chlorophenol under the illumination of 70 W indoor white light (800 × 10² lx) at room temperature. In this context, the synthetic wastewater containing 15 ppm 2-chlorophenol was prepared in the laboratory, and the dose of the photocatalyst was optimized by exposing the suspension having 100 mL of pollutant with varying amounts of CeO₂ photocatalyst (50, 100, 150, and 200 mg) in a glass reactor of 14 cm (diameter) and 2 cm (height) to the indoor white light for 3 h and the samples were collected and filtered using 0.20 μm syringe filter. The filtered samples were then subjected to UV-visible spectrophotometer for the monitoring of photodegradation of 2-CP and 100 mg of the photocatalyst was found to be the optimum dose of catalyst in 100 mL of pollutant. The optimized amount, i.e., 100 mg/100 mL of all four photocatalysts was further used for the evaluation of their photocatalytic degradation efficiency in removing 2-CP under the exposure of 70 W indoor LED white light (800 × 10² lx, 400–800 nm, Oppl Lighting Co., Ltd. China) at room temperature and samples were collected after 30, 60, 90, 120, 180 and 240 min and filter using 0.20 μm syringe filter for UV-visible spectrophotometric analysis to evaluate the kinetic of photodegradation.

To study the removal of the target pollutant from the polluted water, the samples were collected using a syringe filter from the suspension exposed to the light after a regular interval and were subjected to UV-visible spectrophotometer for the determination of the concentration of the removed pollutant which ultimately led to the % removal of target pollutant by the photocatalyst under the exposure of light using the following equation.

$$\% \text{ removal} = \frac{C_o - C_t}{C_o} \times 100 \quad (1)$$

Here, C_o is the pollutant initial concentration whereas C_t is the concentration of the pollutant after exposure time “t.” Moreover, the validity of Langmuir Hinshelwood (L-H) kinetic models was also

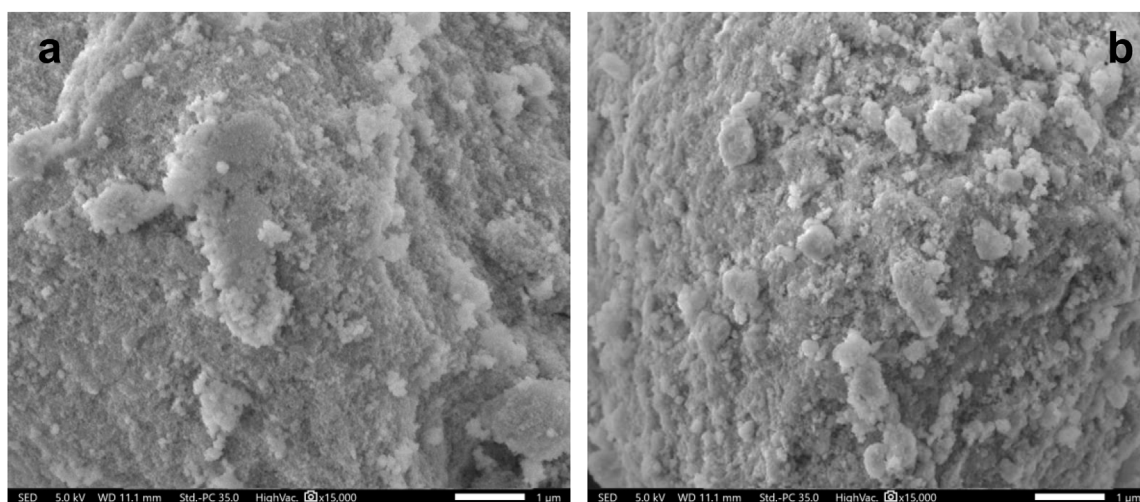


FIGURE 5

The comparison of scanning electron micrographs of (A) pristine CeO_2 and (B) Fe doped CeO_2 .

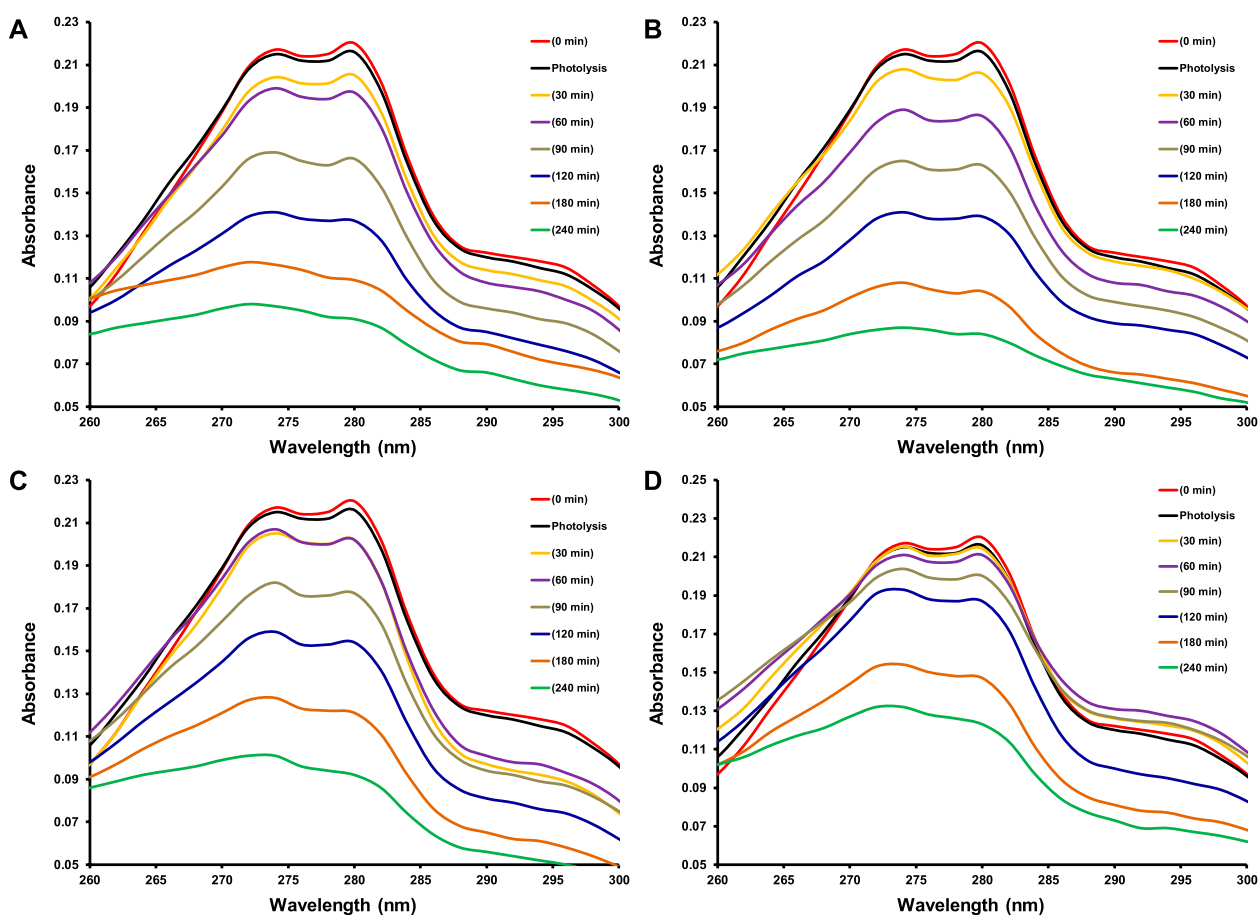
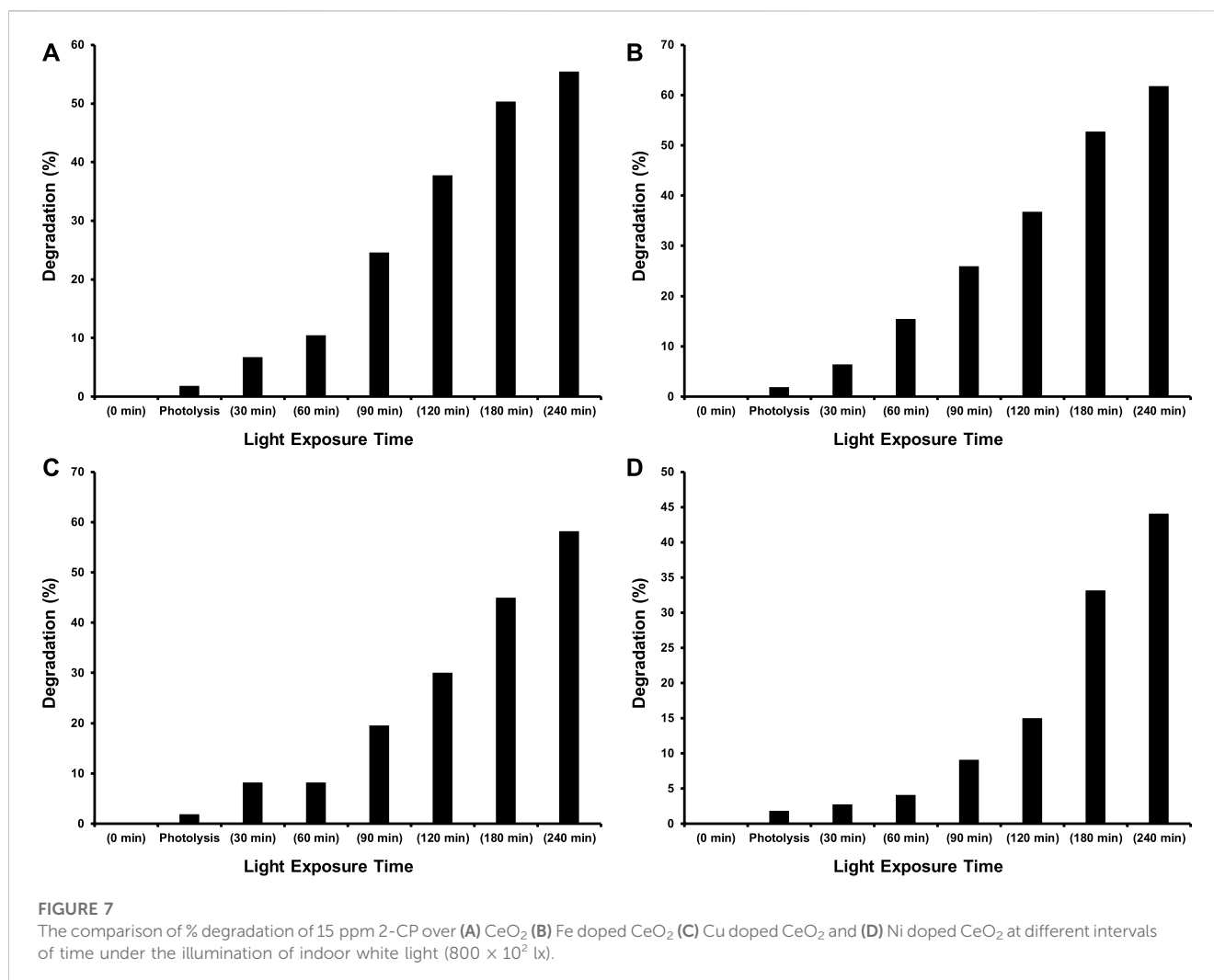


FIGURE 6

The comparison of absorption spectra for photocatalytic degradation of 15 ppm 2-CP over (A) CeO_2 (B) Fe doped CeO_2 (C) Cu doped CeO_2 and (D) Ni doped CeO_2 at different intervals of time under the illumination of indoor white light (800×10^2 lx).



studied using the following equation to evaluate the kinetics of photocatalytic removal of organic pollutants under exposure to light.

$$\ln \frac{C_o}{C_t} = k \times t \quad (2)$$

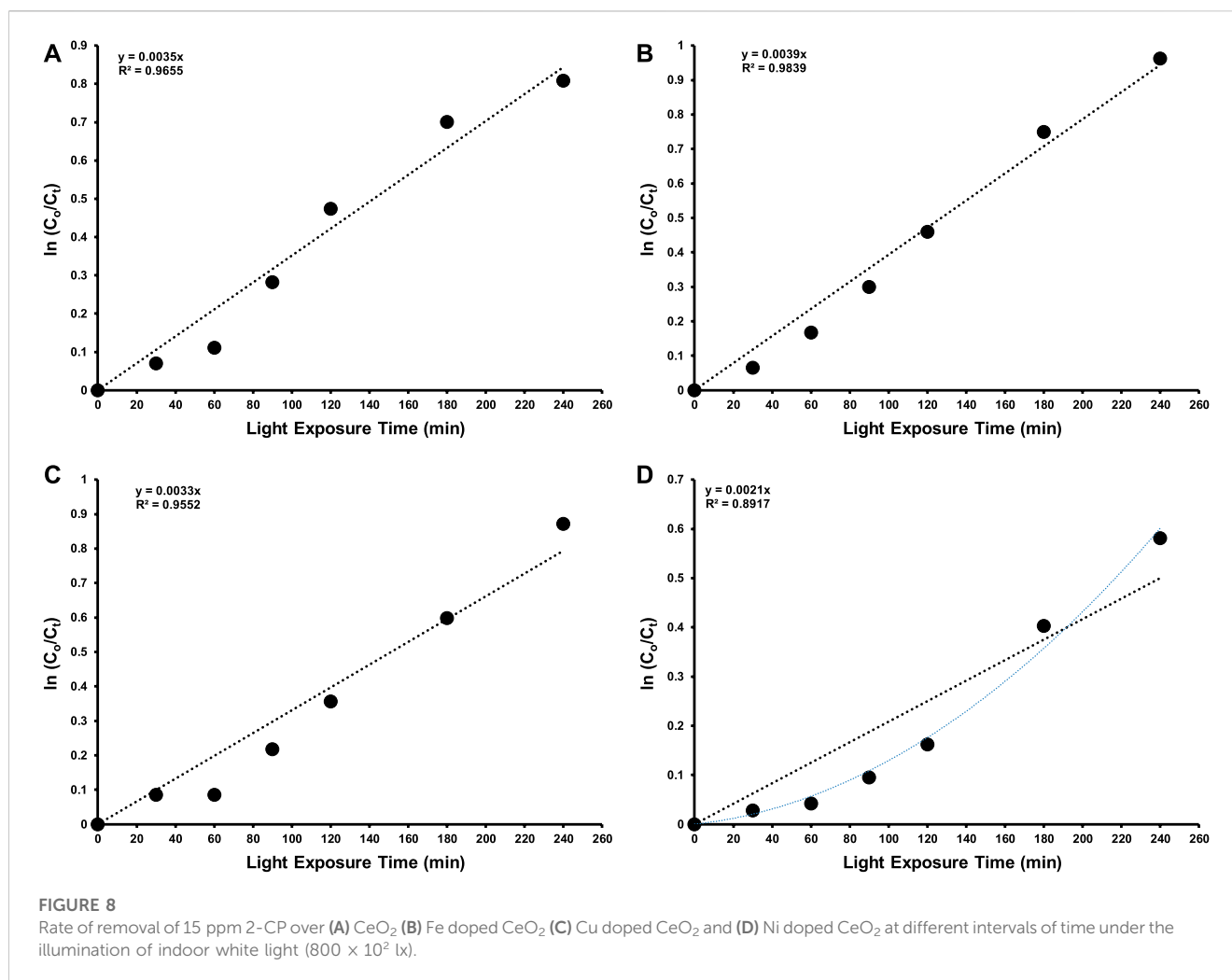
Here, k is the rate constant which was determined from the slope by plotting $\ln \frac{C_o}{C_t}$ Vs. t .

Results and discussion

The solid-state absorption response of the pristine CeO₂ compared to the modified CeO₂ is presented in Figure 1A in UV (200–400 nm) as well as visible (400–800 nm) regions of the spectrum. Wherein, Cu-doped CeO₂ shows higher absorbance in both UV and visible regions than other synthesized materials. Interestingly, Cu-doped CeO₂ and Fe-doped CeO₂ showed higher absorbance of visible light than CeO₂ and Ni-doped CeO₂ whereas in the UV region of the spectrum only Cu-doped CeO₂ presented higher absorbance than other photocatalysts. So, the insertion of Cu and Fe content into the structure of CeO₂ leads to an increase in the

spectral response of CeO₂ whereas the same amount of Ni content has a detrimental effect on the spectral response of the pristine CeO₂. Moreover, the response of these photocatalysts in reflecting the light spectrum has also been explored in Figure 1B. Wherein, lower reflectance (%) was noticed for CeO₂ having copper contents followed by Fe and Ni contents in the lower energy region of the spectrum. This higher absorbance and lower reflectance (%) were attributed to the higher absorbance ability of copper content present in the structure of CeO₂ as compared to Fe and Ni.

The direct and indirect band gap evaluations (Figures 2A, B) reveal a lowering in the band gap energy of Cu and Fe-doped CeO₂ photocatalysts as compared to pristine CeO₂ was noticed which may be attributed to the shifting of conduction band edges to lower energy due to the addition of Cu and Fe contents in the structure of CeO₂ (Yue and Zhang, 2009; Qi et al., 2019). Whereas a significant increase in the band gap energy of Ni-doped CeO₂ was observed. The direct and indirect band gaps of the pristine CeO₂ were noticed at ~3.0 and ~2.9 eV, respectively which have good agreement with the literature values (Aslam et al., 2016). Moreover, the direct band gap energies found for Cu, Fe, and Ni-doped CeO₂ photocatalysts are ~2.85, ~2.8, and ~3.2 eV whereas evaluated indirect band gap energies are ~2.78, ~2.7, and ~3.0 eV, respectively as shown in



Figures 2A, B. A greater decrease in the band gap energy was noticed for Fe doped CeO₂ as compared to other photocatalysts which reveal that this photocatalyst requires lower energy as compared to pristine and other modified photocatalysts to make good use of excitons for the removal of organic toxins under the illumination of light.

Photoluminescence analysis is a promising technique to study the emission intensity of the excited electron under the illumination of light which ultimately leads to the study of e^-h^+ recombination process. Figure 3 depicts the comparison of photoluminescence spectra of pristine and doped CeO₂ photocatalysts, wherein a significantly lower emission intensity was noticed for Cu and Ni-doped CeO₂ as compared to unmodified CeO₂. The relative decrease in emission intensities of the Cu and Fe doped CeO₂ as compared to CeO₂ is strong evidence for lowering e^-h^+ recombination rate than pristine CeO₂ which favors the photocatalytic degradation of organic toxins. Moreover, the decrease in strong emission bands around 470 nm is attributed to the trapping of photoexcitons by the surface defects generated due to the insertion of Cu or Fe into the structure of CeO₂ (George et al., 2020).

The comparison of x-ray diffraction patterns of the modified CeO₂ with pristine CeO₂ is presented in Figure 4 and the cubic phase of the synthesized CeO₂ was confirmed by matching diffractions planes (111), (200), (220), (311), (222), (400), (331), and (420) with

literature and JCPDS 34-0394 (Aslam et al., 2016). The absence of additional diffraction peaks related to the dopant entities in the respective diffraction patterns verifies the successful doping of CeO₂ with Cu, Ni, and Fe. Moreover, few changes such as reduction in few peaks' height, minor peak shift at 2θ (28.525°) and peaks' broadening in XRD patterns of modified CeO₂ as compared to pristine CeO₂ also favour the introduction of dopants in CeO₂ (Kumar et al., 2010). Moreover, the successful insertion of dopants into CeO₂ without significantly altering its structure were also evident from the micrographs as shown in Figure 5. The average crystallite size of the photocatalytic materials was calculated using a high-intensity diffraction peak at 2θ (28.525°) with the help of the Debye-Scherrer equation. The calculated crystallite sizes were 9.76, 3.46, 4.97, and 8.28 nm for pristine CeO₂, Fe doped CeO₂, Cu doped CeO₂, and Ni doped CeO₂, respectively. Moreover, a significant difference in doped CeO₂ as compared to unmodified CeO₂ were also reported in literature which support the changes in crystallite sizes of Fe and Cu doped CeO₂ (Yue and Zhang, 2009; Kumar et al., 2010; Qi et al., 2019).

As this study was designed to investigate the effect of transition metal dopants on the photocatalytic performance of CeO₂ under the illumination of indoor white light for the degradation of 15 ppm 2-CP. Before the exposure of suspension containing photocatalyst

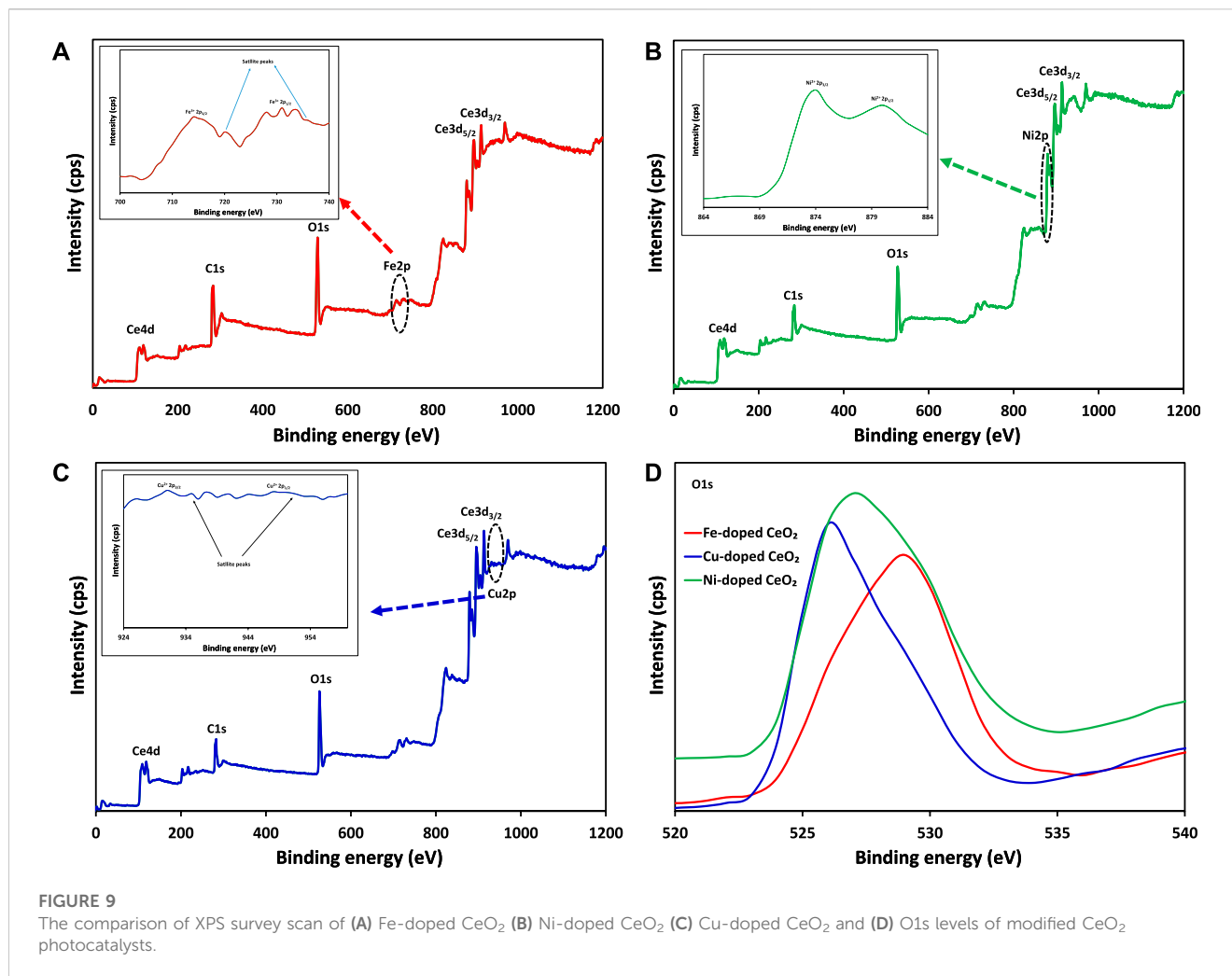


TABLE 1 Agar Well cut diffusion method zone of inhibition for the antifungal action of CeO₂, Fe-doped CeO₂, Ni-doped CeO₂ and Cu-doped CeO₂.

| Antifungal performance | | | |
|------------------------|---------------------------|-------|-------------------------|
| Bacterial strains | Samples | Blank | Zone of inhibition (mm) |
| <i>M. fructicola</i> | CeO ₂ | 0 | 17.4 |
| | Fe-doped CeO ₂ | 0 | 25.3 |
| | Cu-doped CeO ₂ | 0 | 21.1 |
| | Ni-doped CeO ₂ | 0 | 12.2 |
| <i>F. oxysporum</i> | CeO ₂ | 0 | 15.7 |
| | Fe-doped CeO ₂ | 0 | 23.1 |
| | Cu-doped CeO ₂ | 0 | 19.4 |
| | Ni-doped CeO ₂ | 0 | 10.3 |

and 2-CP to light as mentioned in the experimental section, the suspension was kept in dark for 30 min to establish an equilibrium between pollutant and catalyst. The photolysis of 2-CP was also

evaluated by recording the absorption spectrum of the substrate after 240 min of light exposure without the presence of a photocatalyst. The amount of photocatalyst was also optimized

(100 mg of photocatalyst) while studying the photocatalytic removal of 15 ppm 2-CP with varying doses of CeO₂ catalyst under the illumination of indoor white light. The comparison of absorption spectra of photocatalytic removal of 2-CP over pristine CeO₂, Fe doped CeO₂, Cu doped CeO₂, and Ni-doped CeO₂ under the illumination of indoor white light (800 × 102 lx) is provided in Figure 6, respectively at different exposure time. Whereas the photocatalytic degradation (%) of 2-CP at different exposure over the pristine and modified CeO₂ photocatalysts is given in Figure 7, respectively and highest photodegradation (~ 65%) was noticed for Fe doped CeO₂ followed by Cu doped CeO₂ (~ 60%), pure CeO₂ (~59%) and Ni doped CeO₂ (~45%) under the exposure of white light after 240 min of exposure. The decreasing trend of removal efficiency (%) of the photocatalysts is given below.

Fe doped CeO₂ > Cu doped CeO₂ > CeO₂ > Ni doped CeO₂

Moreover, the rate of photodegradation of 15 ppm 2-CP over synthesized photocatalysts was also investigated and higher photocatalytic removal efficiency with rate constant ($k = 3.9 \times 10^{-3} \text{ min}^{-1}$) was observed by Fe doped CeO₂ than others as shown in Figure 8. The calculated bandgap energy values as shown in Figure 2 also support the possible higher photodegradation efficiency of Fe-doped CeO₂ due to its lower bandgap energy than CeO₂. Moreover, a lower photo-excitons' recombination in PL spectra presented by Fe-doped CeO₂ also arguments its higher removal efficiency due to the possible charge transferability for the generation of ROS. The decreasing trend of rate of removal of 2-CP by different photocatalysts is provided below.

Fe doped CeO₂ > CeO₂ > Cu doped CeO₂ > Ni doped CeO₂

The kinetic study also reveals that the photocatalytic removal of 2-CP by Fe doped CeO₂, pure CeO₂, Cu doped CeO₂ followed Langmuir Hinshelwood (L-H) kinetic model whereas the photocatalytic removal of 2-CP by Ni doped CeO₂ did not follow Langmuir Hinshelwood (L-H) kinetic model. Previously, Zhang et al. (2022) reported a decrease in degradation rate of 2-CP removal in the illumination of 5W LED white light as compared to 300 W Xe arc lamp. In another study, BiFeO₃/Bi₂Fe₄O₉ heterojunctions were able to remove 95% of the 2-CP in the exposure of 150W LED white light (Wang et al., 2022).

In this study, x-ray photoelectron spectroscopy (XPS) was also carried out to investigate the chemical and electronic states of the elements in modified materials as shown in Figure 9. The presence of Ce3d_{3/2}, Ce3d_{5/2}, Fe2p_{1/2}, Fe2p_{3/2}, Cu2p_{1/2}, Cu2p_{3/2}, Ni2p_{1/2}, Ni2p_{3/2} core levels and O1s levels in the synthesized photocatalysts can be seen in Figure 9, which confirm the existence of dopants (Fe³⁺, Cu²⁺ and Ni²⁺) in doped CeO₂ as shown in inset figures. Moreover, the effect of dopants was also verified by the appearance of peak correspond to O1s level at different binding energies which ultimately confirm the different environment of oxygen.

Antifungal activity

Using the agar well-diffusion method and amphotericin B as a reference, CeO₂, Fe-doped CeO₂, Ni-doped CeO₂, and Cu-doped

CeO₂ nanoparticles were further assessed for their antifungal activity against *M. fructicola* and *F. oxysporum*. Table 1 provides a summary of the outcomes. According to the antifungal activity data (Table 1), Fe-doped CeO₂ nanoparticles exhibit greater toxicity when compared to CeO₂, Ni-doped CeO₂, and Cu-doped CeO₂ nanoparticles, with zone inhibition values of 25.3 and 23.1 mm. Due to their small particle size, the Fe-doped CeO₂ nanoparticles easily pass through the fungal cell membrane, attach to functional protein groups as well as substances that contain phosphorus and sulphur, including DNA, and ultimately result in fungal cell death. The improved antifungal impact was caused by the synergistic interaction of Fe-doped CeO₂ nanoparticles and decreased size.

Conclusion

In conclusion, cubic CeO₂ was doped successfully with Fe, Cu and Ni through co-precipitation method followed by calcination at 400°C for 4 h. The crystallite sizes were reduced from 9.76 to 3.46 nm by incorporating 3d transition metals into CeO₂. Solid-state absorption analysis revealed a better spectral response and lower bandgap energy of Fe and Cu-doped CeO₂ than unmodified CeO₂ whereas increase in bandgap energy was noticed for Ni-doped CeO₂. Moreover, the insertion of Cu and Fe into CeO₂ suppressed its e⁻-h⁺ recombination process by generating trapping sites for photo-excitons. Among the synthesized photocatalysts in this study, Fe-doped CeO₂ is excellent for the removal of 2-CP in the illumination of 70 W indoor LED white light.

Data availability statement

The original contributions presented in the study are included in the article/supplementary material, further inquiries can be directed to the corresponding authors.

Author contributions

MQ: Conception, design of study, writing-original draft preparation. SI: Interpret the data, performed major experimental works, writing-original draft preparation and editing. MA: He wrote the antifungal analysis part in the manuscript, interpreted the data and critical revision. AA: He wrote the UV-vis application part in the manuscript, interpreted the data and critical revision. ABI: Conception, performed dye degradation analysis, acquisition of data, interpret the data. KR: She wrote the PL analysis part in the manuscript, interpreted the data and critical revision. HF: Performed dye degradation analysis, reviewed original manuscript and critical revision. TS: Reviewed original manuscript, and critical revision. ABa: He performed synthesis methodology. NA: Visualization of data, XRD analysis, funding acquisition, writing reviewing, and editing. HI: Conception, visualization of data, performed bandgap analysis, funding acquisition. RA: She wrote the SEM analysis part in the manuscript, funding acquisition, interpreted the data and critical revision. EE: Visualization of data, reviewed original manuscript and critical revision.

Funding

The authors extend their appreciation to the Deanship of Scientific Research at King Khalid University for supporting this work through research groups program under grant number RGP.2/334/44. The authors thank the Higher Education Commission, Pakistan and Department of Chemistry, Forman Christian College (A Chartered University) Lahore Pakistan for supporting this work by grant No. 21-1865/SRGP/R&D/HEC/2018. This research was funded by Princess Nourah bint Abdulrahman University Researchers Supporting Project number (PNURSP2023R316), Princess Nourah bint Abdulrahman University, Riyadh, Saudi Arabia. The authors extend their appreciation to the Research Center at Almaarefa University for funding this work.

Acknowledgments

The authors extend their appreciation to the Deanship of Scientific Research at King Khalid University for supporting this work through research groups program under grant number RGP.2/334/44. The authors thank the Higher Education Commission, Pakistan and Department of Chemistry, Forman Christian

References

- Adeyemi, A., Göpfert, A., Adeyemi, O. A., and Wolff, T. (2016). Adsorption of 2-chlorophenol onto the surface of underutilized seed of *adenopus breviflorus*: A potential means of treating waste water. *J. Environ. Chem. Eng.* 4 (1), 664–672. doi:10.1016/j.jece.2015.12.012
- Ahmed, S., Rasul, M., Martens, W. N., Brown, R., and Hashib, M. (2010). Heterogeneous photocatalytic degradation of phenols in wastewater: A review on current status and developments. *Desalination* 261 (1–2), 3–18. doi:10.1016/j.desal.2010.04.062
- Alhagbi, B. G., Aslam, M., Hameed, A., and Qamar, M. T. (2020). The efficacy of Co_3O_4 loaded WO_3 sheets for the enhanced photocatalytic removal of 2, 4, 6-trichlorophenol in natural sunlight exposure. *J. Hazard. Mater.* 397, 122835–122843. doi:10.1016/j.jhazmat.2020.122835
- Anku, W. W., Mamo, M. A., and Govender, P. P. (2017). “Phenolic compounds in water: Sources, reactivity, toxicity and treatment methods,” in *Phenolic Compounds - Natural Sources, Importance and Applications*, 419–443. doi:10.5772/66927
- Aslam, M., Qamar, M., Soomro, M. T., Ismail, I. M., Salah, N., Almelbi, T., et al. (2016). The effect of sunlight induced surface defects on the photocatalytic activity of nanosized CeO_2 for the degradation of phenol and its derivatives. *Appl. Catal. B Environ.* 180, 391–402. doi:10.1016/j.apcatb.2015.06.050
- Aslam, M., Qamar, M. T., Ali, S., Rehman, A. U., Soomro, M., Ahmed, I., et al. (2018). Evaluation of SnO_2 for sunlight photocatalytic decontamination of water. *J. Environ. Manag.* 217, 805–814. doi:10.1016/j.jenvman.2018.04.042
- Barakat, M., Kumar, R., Rashid, J., Seliem, M. K., Al-Mur, B., and El-Shishtawy, R. M. (2020). A novel $\text{CuO-Cu}_2\text{O/Ag-Ag}_3\text{PO}_4$ nanocomposite: Synthesis, characterization, and its application for 2-chlorophenol decontamination under visible light. *J. Taiwan Inst. Chem. Eng.* 115, 208–217. doi:10.1016/j.jtice.2020.10.030
- Brillas, E., and Garcia-Segura, S. (2020). Benchmarking recent advances and innovative technology approaches of fenton, photo-fenton, electro-fenton, and related processes: A review on the relevance of phenol as model molecule. *Sep. Purif. Technol.* 237, 116337–116367. doi:10.1016/j.seppur.2019.116337
- Chiou, C.-H., Wu, C.-Y., and Juang, R.-S. (2008). Photocatalytic degradation of phenol and m-nitrophenol using irradiated TiO_2 in aqueous solutions. *Sep. Purif. Technol.* 62 (3), 559–564. doi:10.1016/j.seppur.2008.03.009
- Danish, M. S. S., Estrella, L. L., Alemáida, I. M. A., Lisin, A., Moiseev, N., Ahmadi, M., et al. (2021). Photocatalytic applications of metal oxides for sustainable environmental remediation. *Metals* 11 (1), 80–104. doi:10.3390/met11010080
- Du, X., and Zhou, M. (2021). Strategies to enhance catalytic performance of metal-organic frameworks in sulfate radical-based advanced oxidation processes for

College (A Chartered University) Lahore Pakistan for supporting this work by grant No. 21-1865/SRGP/R&D/HEC/2018. This research was funded by Princess Nourah bint Abdulrahman University Researchers Supporting Project number (PNURSP2023R316), Princess Nourah bint Abdulrahman University, Riyadh, Saudi Arabia. The authors extend their appreciation to the Research Center at Almaarefa University for funding this work.

Conflict of interest

The authors declare that the research was conducted in the absence of any commercial or financial relationships that could be construed as a potential conflict of interest.

Publisher's note

All claims expressed in this article are solely those of the authors and do not necessarily represent those of their affiliated organizations, or those of the publisher, the editors and the reviewers. Any product that may be evaluated in this article, or claim that may be made by its manufacturer, is not guaranteed or endorsed by the publisher.

- organic pollutants removal. *Chem. Eng. J.* 403, 126346–126361. doi:10.1016/j.cej.2020.126346
- Elias, J. S., Risch, M., Giordano, L., Mansour, A. N., and Shao-Horn, Y. (2014). Structure, bonding, and catalytic activity of monodisperse, transition-metal-substituted CeO_2 nanoparticles. *J. Am. Chem. Soc.* 136 (49), 17193–17200. doi:10.1021/ja509214d
- Eryilmaz, C., and Genç, A. (2021). Review of treatment technologies for the removal of phenol from wastewaters. *J. Water Chem. Technol.* 43 (2), 145–154. doi:10.3103/s1063455x21020065
- Fauzi, A., Jalil, A., Hassan, N., Aziz, F., Azami, M., Hussain, I., et al. (2022). A critical review on relationship of CeO_2 -based photocatalyst towards mechanistic degradation of organic pollutant. *Chemosphere* 286, 131651. doi:10.1016/j.chemosphere.2021.131651
- Gallo-Cordova, A., Veintemillas-Verdaguer, S., Tartaj, P., Mazarío, E., Morales, M. d. P., and Ovejero, J. G. (2021). Engineering iron oxide nanocatalysts by a microwave-assisted polyol method for the magnetically induced degradation of organic pollutants. *Nanomaterials* 11 (4), 1052–1068. doi:10.3390/nano11041052
- García-Hernández, L. E., Frías-Márquez, D. M., Pacheco-Sosa, J. G., Cervantes-Urribe, A., Arévalo-Pérez, J. C., Pérez-Vidal, H., et al. (2019). 2-Chlorophenol degradation by catalytic wet air oxidation using copper supported on $\text{TiO}_2\text{-CeO}_2\text{-ZrO}_2$. *Water Sci. Technol.* 80 (5), 911–919. doi:10.2166/wst.2019.330
- George, S. E., George, M., Alex, J., Joy, L. K., Aravind, A., Sajan, D., et al. (2020). Nonlinear optical and photocatalytic dye degradation of Co doped CeO_2 nanostructures synthesized through a modified combustion technique. *Ceram. Int.* 46 (9), 13932–13940. doi:10.1016/j.ceramint.2020.02.189
- Gisbertz, S., and Pieber, B. (2020). Heterogeneous photocatalysis in organic synthesis. *ChemPhotoChem* 4 (7), 454–475. doi:10.1002/cptc.202000137
- Hao, C., Li, J., Zhang, Z., Ji, Y., Zhan, H., Xiao, F., et al. (2015). Enhancement of photocatalytic properties of TiO_2 nanoparticles doped with CeO_2 and supported on SiO_2 for phenol degradation. *Appl. Surf. Sci.* 331, 17–26. doi:10.1016/j.apsusc.2015.01.069
- Huang, B., Wu, Z., Zhou, H., Li, J., Zhou, C., Xiong, Z., et al. (2021). Recent advances in single-atom catalysts for advanced oxidation processes in water purification. *J. Hazard. Mater.* 412, 125253–125273. doi:10.1016/j.jhazmat.2021.125253
- Kanan, S., Moyet, M. A., Arthur, R. B., and Patterson, H. H. (2020). Recent advances on TiO_2 -based photocatalysts toward the degradation of pesticides and major organic pollutants from water bodies. *Catal. Rev.* 62 (1), 1–65. doi:10.1080/01614940.2019.1613323
- Kumar, S., Kim, Y. J., Koo, B., and Lee, C. G. (2010). Structural and magnetic properties of Ni doped CeO_2 nanoparticles. *J. Nanosci. Nanotechnol.* 10 (11), 7204–7207. doi:10.1166/jnn.2010.2751

- Loeb, S. K., Alvarez, P. J., Brame, J. A., Cates, E. L., Choi, W., Crittenden, J., et al. (2019). The technology horizon for photocatalytic water treatment: Sunrise or sunset? *Environ. Sci. Technol.* 53 (6), 2937–2947. doi:10.1021/acs.est.8b05041
- Luo, H., Zeng, Y., He, D., and Pan, X. (2021). Application of iron-based materials in heterogeneous advanced oxidation processes for wastewater treatment: A review. *Chem. Eng. J.* 407, 127191–127213. doi:10.1016/j.cej.2020.127191
- Ma, R., Zhang, S., Wen, T., Gu, P., Li, L., Zhao, G., et al. (2019). A critical review on visible-light-response CeO₂-based photocatalysts with enhanced photooxidation of organic pollutants. *Catal. today* 335, 20–30. doi:10.1016/j.cattod.2018.11.016
- Mazivila, S. J., Ricardo, I. A., Leitão, J. M., and da Silva, J. C. E. (2019). A review on advanced oxidation processes: From classical to new perspectives coupled to two- and multi-way calibration strategies to monitor degradation of contaminants in environmental samples. *Trends Environ. Anal. Chem.* 24, e00072–e00081. doi:10.1016/j.teac.2019.e00072
- Oturan, M. A., and Aaron, J.-J. (2014). Advanced oxidation processes in water/wastewater treatment: Principles and applications. A review. *Crit. Rev. Environ. Sci. Technol.* 44 (23), 2577–2641. doi:10.1080/10643389.2013.829765
- Pandey, S., Mandari, K. K., Kim, J., Kang, M., and Fosso-Kankeu, E. (2020). Recent advancement in visible-light-responsive photocatalysts in heterogeneous photocatalytic water treatment technology. *Photocatal. Adv. Oxid. Process. wastewater Treat.*, 167–196. doi:10.1002/9781119631422.ch6
- Qamar, M. T., Aslam, M., Ismail, I. M., Salah, N., and Hameed, A. (2015). Synthesis, characterization, and sunlight mediated photocatalytic activity of CuO coated ZnO for the removal of nitrophenols. *ACS Appl. Mater. interfaces* 7 (16), 8757–8769. doi:10.1021/acsami.5b01273
- Qamar, M. T., Aslam, M., Rehan, Z., Soomro, M. T., Basahi, J. M., Ismail, I. M., et al. (2017). The influence of p-type Mn₃O₄ nanostructures on the photocatalytic activity of ZnO for the removal of bromo and chlorophenol in natural sunlight exposure. *Appl. Catal. B Environ.* 201, 105–118. doi:10.1016/j.apcatb.2016.08.004
- Qamar, M., Aslam, M., Rehan, Z., Soomro, M., Basahi, J. M., Ismail, I. M., et al. (2017). The effect of Fe³⁺ based visible light receptive interfacial phases on the photocatalytic activity of ZnO for the removal of 2, 4-dichlorophenoxy acetic acid in natural sunlight exposure. *Sep. Purif. Technol.* 172, 512–528. doi:10.1016/j.seppur.2016.08.030
- Qi, Y., Ye, J., Zhang, S., Tian, Q., Xu, N., Tian, P., et al. (2019). Controllable synthesis of transition metal ion-doped CeO₂ micro/nanostructures for improving photocatalytic performance. *J. Alloys Compd.* 782, 780–788. doi:10.1016/j.jallcom.2018.12.111
- Rafiq, A., Ikram, M., Ali, S., Niazi, F., Khan, M., Khan, Q., et al. (2021). Photocatalytic degradation of dyes using semiconductor photocatalysts to clean industrial water pollution. *J. Indust. Eng. Chem.* 2021, 1–18. doi:10.1016/j.jiec.2021.02.017
- Rashid, J., Parveen, N., Iqbal, A., Awan, S. U., Iqbal, N., Talib, S. H., et al. (2019). Facile synthesis of g-C₃N₄ (0.94)/CeO₂ (0.05)/Fe₃O₄ (0.01) nanosheets for DFT supported visible photocatalysis of 2-Chlorophenol. *Sci. Rep.* 9 (1), 10202. doi:10.1038/s41598-019-46544-7
- Ren, G., Han, H., Wang, Y., Liu, S., Zhao, J., Meng, X., et al. (2021). Recent advances of photocatalytic application in water treatment: A review. *Nanomaterials* 11 (7), 1804–1825. doi:10.3390/nano11071804
- Samanta, P., Desai, A. V., Let, S., and Ghosh, S. K. (2019). Advanced porous materials for sensing, capture and detoxification of organic pollutants toward water remediation. *ACS Sustain. Chem. Eng.* 7 (8), 7456–7478. doi:10.1021/acssuschemeng.9b00155
- Saputera, W. H., Putrie, A. S., Esmailpour, A. A., Sasongko, D., Suendo, V., and Mukti, R. R. (2021). Technology advances in phenol removals: Current progress and future perspectives. *Catalysts* 11 (8), 998–1042. doi:10.3390/catal11080998
- Serrà, A., and Philippe, L. (2020). Simple and scalable fabrication of hairy ZnO@ZnS core@shell Cu cables for continuous sunlight-driven photocatalytic water remediation. *Chem. Eng. J.* 401, 126164–126172. doi:10.1016/j.cej.2020.126164
- Sharma, G., Kumar, A., Naushad, M., Sharma, S., Ghfar, A. A., Ahamad, T., et al. (2019). Graphene oxide supported La/Co/Ni trimetallic nano-scale systems for photocatalytic remediation of 2-chlorophenol. *J. Mol. Liq.* 294, 111605–111614. doi:10.1016/j.molliq.2019.111605
- Tang, J., Zou, Z., and Ye, J. (2004). Efficient photocatalytic decomposition of organic contaminants over CaBi₂O₄ under visible-light irradiation. *Angew. Chem.* 116 (34), 4463–4466. doi:10.1002/anie.200353594
- Umukoro, E. H., Peleyeye, M. G., Ngila, J. C., and Arotiba, O. A. (2017). Towards wastewater treatment: Photo-assisted electrochemical degradation of 2-nitrophenol and orange II dye at a tungsten trioxide-exfoliated graphite composite electrode. *Chem. Eng. J.* 317, 290–301. doi:10.1016/j.cej.2017.02.084
- Wang, M., Iocozzia, J., Sun, L., Lin, C., and Lin, Z. (2014). Inorganic-modified semiconductor TiO₂ nanotube arrays for photocatalysis. *Energy & Environ. Sci.* 7 (7), 2182–2202. doi:10.1039/c4ee00147h
- Wang, Y., Tang, Y., Sun, J., Wu, X., Liang, H., Qu, Y., et al. (2022). BiFeO₃/Bi₂Fe₄O₉ S-scheme heterojunction hollow nanospheres for high-efficiency photocatalytic o-chlorophenol degradation. *Appl. Catal. B Environ.* 319, 121893. doi:10.1016/j.apcatb.2022.121893
- Xu, J., Wang, Z., and Zhu, Y. (2017). Enhanced visible-light-driven photocatalytic disinfection performance and organic pollutant degradation activity of porous g-C₃N₄ nanosheets. *ACS Appl. Mater. interfaces* 9 (33), 27727–27735. doi:10.1021/acsami.7b07657
- Yao, J., Gao, Z., Meng, Q., He, G., and Chen, H. (2021). One-step synthesis of reduced graphene oxide based ceric dioxide modified with cadmium sulfide (CeO₂/CdS/RGO) heterojunction with enhanced sunlight-driven photocatalytic activity. *J. Colloid Interface Sci.* 594, 621–634. doi:10.1016/j.jcis.2021.03.034
- Yue, L., and Zhang, X.-M. (2009). Structural characterization and photocatalytic behaviors of doped CeO₂ nanoparticles. *J. Alloys Compd.* 475 (1–2), 702–705. doi:10.1016/j.jallcom.2008.07.096
- Zangeneh, H., Zinatizadeh, A., Habibi, M., Akia, M., and Isa, M. H. (2015). Photocatalytic oxidation of organic dyes and pollutants in wastewater using different modified titanium dioxides: A comparative review. *J. Indust. Eng. Chem.* 26, 1–36. doi:10.1016/j.jiec.2014.10.043
- Zhang, L., Zhai, T., Yang, M., and Hu, C. (2022). Few-layered Bi₄O₅I₂ nanosheets enclosed by {1 0–1} facets with oxygen vacancies for highly-efficient removal of water contaminants. *J. Hazard. Mater.* 437, 129274. doi:10.1016/j.jhazmat.2022.129274